Quasi-in-plane leaky modes in lasing cholesteric liquid crystal cells

Lev M. Blinov,[1,a] Gabriella Cipparrone,[2] Alfredo Mazzulla,[2] Pasquale Pagliusi,[2] Vladimir V. Lazarev,[3] and Serguei P. Palto[3]

[1]*LICRYL-CEMIF.CAL, Department of Physics, University of Calabria, 87046 Rende, Cosenza, Italy and Institute of Crystallography, Russian Academy of Sciences, Leninsky prospect 59, 119333 Moscow, Russia*
[2]*LICRYL CNR-CEMIF.CAL, Department of Physics, University of Calabria, 87046 Rende, Cosenza, Italy*
[3]*Institute of Crystallography, Russian Academy of Sciences, Leninsky prospect 59, 119333 Moscow, Russia*

Using a planar cell consisting of a prism and a flat glass, we have carried out precise measurements of the angles at which quasi-in-plane leaky (QIPL) laser modes propagate within a thin layer of a cholesteric liquid crystal (CLC) doped with a laser dye. Both the prism and the glass have refraction indices higher than relevant CLC indices, therefore, the waveguide effect in CLC is excluded. For this type of almost thresholdless lasing neither mirrors nor distributed feedback is necessary. The modes are generated in the amplifying CLC layer due to strong Fresnel reflections from the glass boundaries at propagation angles very close to 90° with respect to the cell normal. In the experiment, two modes polarized differently (*s*- and *p*-) have been found outgoing from the prism. Using equivalency between optical properties of a CLC and optically negative nematic liquid crystal at the propagation angles close to 90°, the analytical approach known for a uniform nematic liquid crystal was used for calculations of the threshold gain of the QIPL modes in a helical CLC. The gain has been found for the particular eigenmodes whose propagation angles have been measured. The experimental and calculated data on the propagation angles, polarization and threshold gain are in quantitative agreement. © *2008 American Institute of Physics.* [DOI: 10.1063/1.2975971]

I. INTRODUCTION

Cholesteric liquid crystals (CLCs) are chiral structures[1] with a value of the helical pitch P comparable to the wavelength λ of visible light. Their optical anisotropy $\Delta n = n_\parallel - n_\perp$ is very high, about 0.1–0.2 (here, $n_\parallel$ and $n_\perp$ are the refraction indices parallel and perpendicular to the director L (preferable direction of the molecular axis). The vector $L(\mathbf{r})$ coincides with the local optical axis rotating in space. This rotation results in a strong modulation of refraction index along the helical axis. Therefore, along this direction, a CLC is a one-dimensional photonic structure with a stop-band position centered at $\lambda_{\text{Bragg}} = \langle n \rangle P$ determined by $\langle n \rangle = (n_\parallel + n_\perp)/2$ and the half-pitch $P/2$. The width of the stop band is determined by Δn. When a laser dye with proper luminescence spectrum is introduced in a CLC, upon pumping, a laser emission is observed at the edges of the stop band. A growing interest in lasing effects in CLC (Refs. 2 and 3) is stimulated by the prospects for building compact, low threshold, and distributed feedback (DFB) lasers with tunability and high sensitivity to various external factors.[4–6]

Moreover, using the electric field one can switch on and off the lasing effect,[7] therefore, thin-film CLC lasers may, in principle, be integrated within a unique multipixel structure pumped in parallel with a series of pulses of a powerful standard laser. Then the outgoing multiple CLC laser beams would transfer a large volume of information. To this effect, one should expand the pump beam cross section; however, the latter creates a problem of aspect ratio of a CLC laser.

Indeed, if the width of the pump area w considerably exceeds the thickness of the CLC laser layer $d \leq 100$ μm, the light would be much stronger amplified in the lateral, quasi-in-plane direction according to the factor $\exp(\alpha w)$, where α is the gain coefficient of the pumped CLC. Eventually the light energy would leak out of the CLC cell guided by the limiting glasses. Even lasing is observed on such quasi-in-plane leaky (QIPL) modes due to the feedback owed to very oblique reflections from the liquid crystal-glass interfaces.[8] The direction of such lasing is almost perpendicular to the helical axis and the Bragg reflection mechanism does not work. It has been shown that in CLC the major part of the laser energy can be carried off by the QIPL modes.[9] The same undesirable effect could be very important for other DFB lasers using thin-film stack photonic structures, e.g., prepared by a holographic technique.[10] On the other hand, electric field controlled lasing on the QIPL modes may be used in planar, e.g., waveguiding, devices.[8]

The theory of leaky modes has been discussed for both spontaneous[11] and laser emission.[12] In Ref. 12 the threshold gain coefficient for lasing in the Fabry–Pérot structure has calculated analytically for an isotropic liquid and nematic liquid crystal with director perpendicular to the glass substrates. It has been shown that the QIPL lasing modes are, in fact, thresholdless. The previous experiments,[8,9] however, have been made rather qualitatively using planar capillary cells formed by two thin glasses. In such cells, it was impossible to make accurate measurements of the angles between the cell interfaces and propagating QIPL beams. The polarization properties of different laser beams outgoing from the two glasses have not been studied either. Therefore, it was

---

impossible to find the structure of the eigenmodes propagating within the liquid crystal material (before they leak out) and compare the experimental results with the theoretical ones.

In the present paper, we use a CLC layer limited by a prism with well-known refraction index at one boundary and a glass plate with approximately same index at the other boundary. By screening either the prism or the glass edges the outgoing laser beams can be analyzed separately. As a result, we have obtained quantitative data for comparison with the theory. The plan of the paper is as follows. In the beginning we present the experimental results. Then, using modeling based on the precise solutions of the Maxwell equations, we show that for the QIPL modes an optically negative (macroscopically) CLC with a helical structure would be indistinguishable from the uniform structure of an optically negative uniaxial nematic liquid crystal, if the refraction indices for the *s*- and *p*-polarized beams for both materials are correspondingly the same. Next, we calculate the threshold gain coefficient for our CLC with the helical axis parallel to the cell normal using the analytic theory developed for a uniform, homeotropically oriented nematic.[12] Then we find the propagation angles, polarization, and gain for the QIPL eigenmodes in the CLC Fabry–Pérot cell and, finally, compare the calculated data with the experimental ones. A good quantitative agreement between the two is shown.

II. EXPERIMENTAL

A. Material and cell

The dye-doped chiral nematic mixture (i.e., CLC) consists of a 76% commercial nematic liquid crystal MLC6815 (Merck) and 24% chiral compound ZLI811 (Merck) doped with 0.5% dye 4-(dicyanomethylene)-2-methyl-6-(4-dimethylamino-styryl)-4*H*-pyran (DCM) (Aldrich). The principal refraction indices of the mixture $n_{\parallel} \approx 1.534$ and $n_{\perp} \approx 1.478$ at $\lambda \cong 550$ nm were found from the refractometric data. The photonic band gap position is seen in the luminescence spectrum in Fig. 1 and located between 595 and 620 nm (observed along the helical axis). The helical pitch calculated from the spectral data and the refraction indices is $P \approx 400 \pm 5$ nm at 22–27 °C. The absorption spectrum of DCM is located within a range of 400–550 nm (see Fig. 1 in Ref. 9).

All experiments have been carried out on a planar capillary cell formed by an equilateral prism and glass plate (see Fig. 2). The inner cell surfaces were covered with thin polyimide layers and unidirectionally rubbed to provide homogeneous planar anchoring a CLC at the interfaces. A quite wide gap ($d = 48$ μm) between the prism and the glass determining the CLC layer thickness was chosen to reduce lasing threshold in the Bragg regime. In this case, we are able to observe the Bragg and QIPL modes at the same rather low pump beam fluence. The gap was filled with the chiral mixture in the isotropic phase. During and after slow cooling to room temperature, the glass was gently shifted to provide a good quality shear-induced planar cholesteric texture with the helical axis $\mathbf{h} \parallel z$. Then the glass was fixed. The refraction
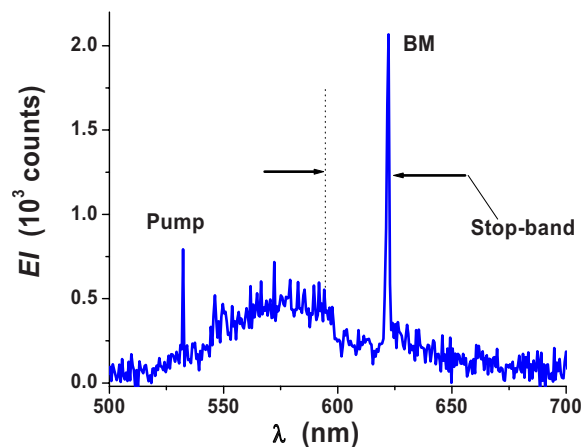

FIG. 1. (Color online) The luminescence spectrum of the CLC material showing the stop-band position. The pump beam is at the angle of $\theta = 45°$ with respect to the cell normal, the detector collects the emission along the cell normal. The pump pulse energy is 23 μJ (fluence $W_p = 0.29$ mJ/cm^2). Lasing on the Bragg mode (BM) is seen at $\lambda = 622.3$ nm.

indices of the prism and glass are $n_p = 1.5151$ (at $\lambda = 589$ nm) and $n_g \approx 1.51$, respectively. It is important that both indices are larger than the CLC indices for the *s*- and *p*-waves propagating in the cell plane *xz* with electric vector either along *y* (*s*-polarization) or lying in the *xz*-plane (*p*-polarization): $n_s = (n_{\parallel} + n_{\perp})/2 = 1.5057 < 1.51$ and n_p depend on the propagation angle, $1.478 = n_{\perp} \leq n_p \leq n_s$. Therefore, in this cell the waveguiding regime is impossible and all eigenwaves propagating in the cell are leaky modes.

B. Measurements

We measured the polarization emission spectra as functions of pump energy and an angle ϕ of the detector position with respect to the *z*-axis. The top view of the experimental
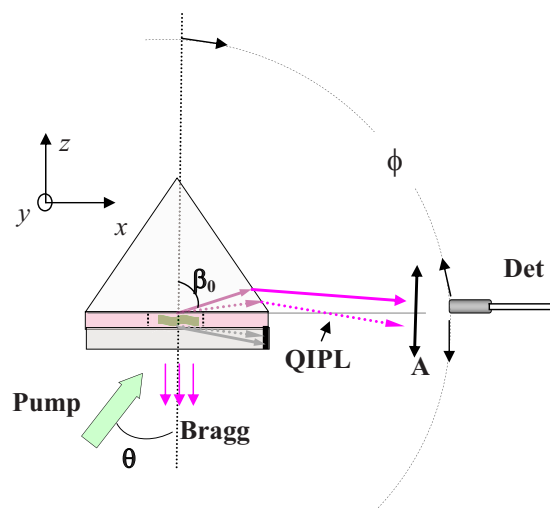

FIG. 2. (Color online) The scheme of experiment and definition of ϕ, β_0, and θ angles (a top view on the laser table). The dye-doped CLC is between a prism and a glass. Upon pumping, CLC emits light in the BM along the cell normal (the second mode propagating into the prism is not shown) and in four QIPL modes propagating to the right (the other four modes propagating to the left are not shown). The two leaky modes within the glass are blocked by a small screen. The detector fiber (Det) equipped with an analyzer (a) can rotate about the cell. The half-base of the prism in the *x*-direction is 12.5 mm, the trajectory radius of the detector input is 45 mm.

scheme is shown in Fig. 2. The cell was installed on a rotating stage and the CLC layer plane (x, y) was adjusted to be vertical. The pump beam was directed either along z or at $\theta = 45°$ with respect to z. The second case shown in the picture is more convenient for observation of lasing in the Bragg mode (BM). The emission spectra were measured upon rotation of the input of a light collecting fiber (Det) through angle ϕ around the vertical axis y, which passes through the middle of the pumped area. We could simultaneously measure an intensity of both the BM (along the z-axis, $\phi = 180°$) and any leaky modes, including the QIPL modes close to the x-axis ($\phi \approx 80° - 90°$). An analyzer was installed between the cell and the fiber connected to an AvaSpec-2048 charge coupled device spectrometer.

The cell was pumped by the second harmonic of a Q-switched Nd:YAG (Y–Al garnet) laser (Continuum, Surelite-II) (wavelength $\lambda = 532$ nm, pulse duration $t_p = 7$ ns, repetition rate 5 Hz). The pump beam was focused into a rectangular, 0.8 mm wide spot (along y) by a cylindrical lens with a focus distance $f = 220$ mm. The length of the spot (along x) was either 7 mm (at $\theta = 0$) or 10 mm at $\theta = 45°$. The pump pulse energy was controlled by calibrated neutral filters and a rotating Glan polarizer. The pulse energy was measured by a power/energy meter (Spectra Physics, model 70260).

C. Experimental results

With increasing pump beam energy, at first, we observe lasing from the edge of the cell and then in the BM. The threshold pump fluence is $W_p \approx 0.13$ mJ/cm^2 (for a QIPL mode) and 0.29 mJ/cm^2 (for the BM). The corresponding threshold pump pulse energies are 10 and 23 μJ/pulse. The BM is generated as a single spectral line at $\lambda = 622.3$ nm (seen in Fig. 1) and could be detected in the angular range of about $\pm 15°$ centered at $\phi = 180°$ (see Fig. 2). Such a wide angular range is a consequence of the x-elongated pump spot form. Further, eight QIPL modes are observed from both edges of the cell. For simplicity, in Fig. 2 only four modes are shown on the right side of the cell. Screening either the glass butt or the right face of the prism we have found that one pair of modes exits from the glass and the other one from the prism. In each pair, one mode is vertically polarized (s-mode) and the other horizontally polarized (p-mode). The angles of the two modes exiting from the glass are not of our interest because they suffer from multiple reflections within the 0.8 mm thick glass. Throughout the paper, we only deal with the beams outgoing from the prism.

The angular dependence of the emission intensity (EI) for the two QIPL modes exiting from the prism is shown in Fig. 3. In this case the pump beam is incident normally onto the cell. The curve was taken without an analyzer, although the polarization state of the emission was controlled in several angular points. We see only two strong peaks located at $\phi = 93.5 \pm 0.5°$ (s-polarized) and $\phi = 84.5 \pm 0.5°$ (p-polarized). The degree of polarization can be deduced from the polarization emission spectra in Fig. 4 presented for two angular positions of the analyzer axis, vertical (s) and horizontal (p). The curves in the upper and lower plots were
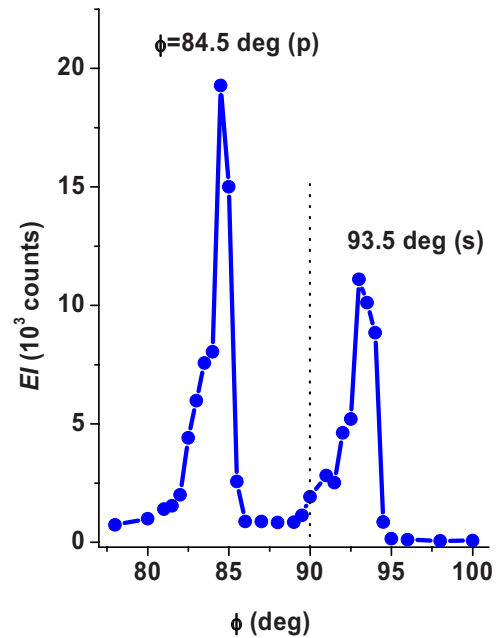
FIG. 3. (Color online) Angular dependence of the EI $\lambda = 608.6$ nm of the QIPL modes exiting from the prism (measured without analyzer). Vertical dotted line corresponds to the base of the prism (in the zy-plane). Pump fluence $W_p = 0.63$ mJ/cm^2.

measured at $\phi = 93.5°$ and $84.5°$, respectively. The degree of polarization is very high. In fact both beams are polarized linearly. In Fig. 4 we also see a multimode structure. However, for the oblique pump beam incidence, at a certain pump fluence we were able to observe a single mode lasing at $\lambda = 606.2$ nm with line width of 1.7 nm limited by the spectrometer resolution. We shall come back to the multimode structure later on.
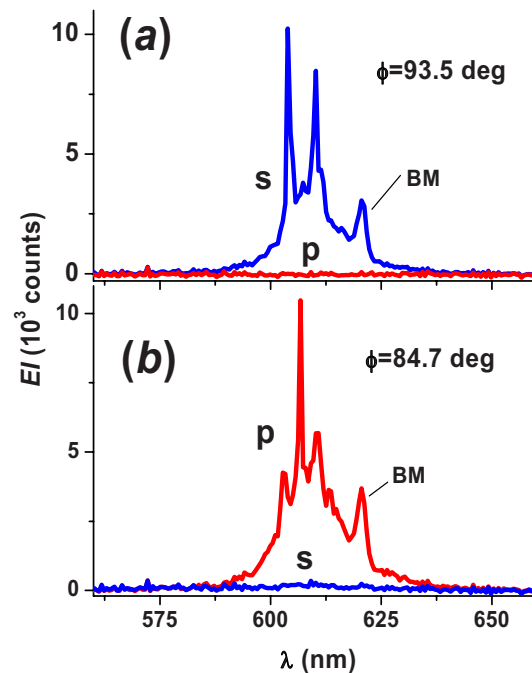
FIG. 4. (Color online) QIPL modes EI spectra measured in polarized light for two angular positions of the detector, $\phi = 93.5°$ (upper plot) and $\phi = 84.5°$ (lower plot). In both cases, the angular position of an analyzer is either vertical (curves s) or horizontal (curves p). Pump fluence in both cases is $W_p = 0.63$ mJ/cm^2. BM is the scattered emission of BM generated at the same pump fluence.
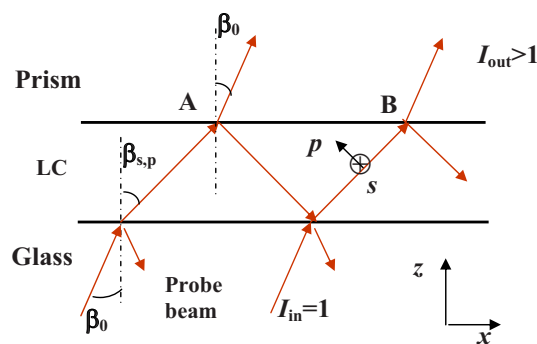
FIG. 5. (Color online) The Fabry–Pérot cell for the simulation. Liquid crystal is an amplifying medium between a glass and a prism, which is either helical CLC or uniform nematic, both optically negative. $I_{in}=1$ is a probe beam with unit intensity, the amplified transmission is AT$=I_{out}/I_{in}.\beta_{s,p}$ are the angles of propagation of the amplified beams for two principle directions (s and p) of the electric vector.

From the measured angles ϕ, using the Snell law and the refraction index of the prism we find the angles β_0, which the two strong beams propagating within the prism form with the z-axis. Therefore our key experimental result, which allows the further discussion of the QIPL eigenmodes in the CLC layer, is as follows:

(a)   a linearly s-polarized beam propagates in the prism at an angle of $\beta_0(s)=83.4\pm0.4°$ and

(b)   a linearly p-polarized beam propagates in the prism at an angle of $\beta_0(p)=77.4\pm0.4°$.

In both cases, the threshold fluence is about of 0.13 mJ/cm^2.

III. COMPARISON OF THE CHOLESTERIC AND AN OPTICALLY NEGATIVE NEMATIC LIQUID CRYSTAL

In this section, we show that for large angles of light incidence, the macroscopically uniaxial, optically negative, and planar helical structure of a CLC is strictly equivalent to a uniform, optically negative, and uniaxial structure of a nematic liquid crystal, like a nematic with disk-shape molecules and $n_\parallel < n_\perp$. In both cases, the unique symmetry axis of the two liquid crystals to be compared is oriented perpendicularly to the cell boundaries. The result of this comparison is very important and can be applied to other one-dimensional photonic structures because it is much simpler to treat theoretically a uniform medium than the stratified or helical one. In our particular case, based on this comparison, we have succeeded in applying the analytical calculation of gain coefficient for a homeotropically oriented nematic[12] to the discussion of the QIPL modes in our helical CLC.

The comparison is made using a software based on the precise solution of the Maxwell equations for the light propagating in a layer of an anisotropic (and chiral) medium confined between two semi-infinite isotropic media.[13,14] The lasing properties of the medium are modeled by an anisotropic negative absorption coefficient α (i.e., positive gain $-\alpha$ in μm^{-1} units). Figure 5 shows the scheme of the simulations. A probe beam of a unit intensity $I=1$ impinges on the liquid crystal layer from the glass at angle β_0, then, partially reflected, propagates in the liquid crystalline amplifying layer at angle β_s or β_p depending on polarization. The amplified
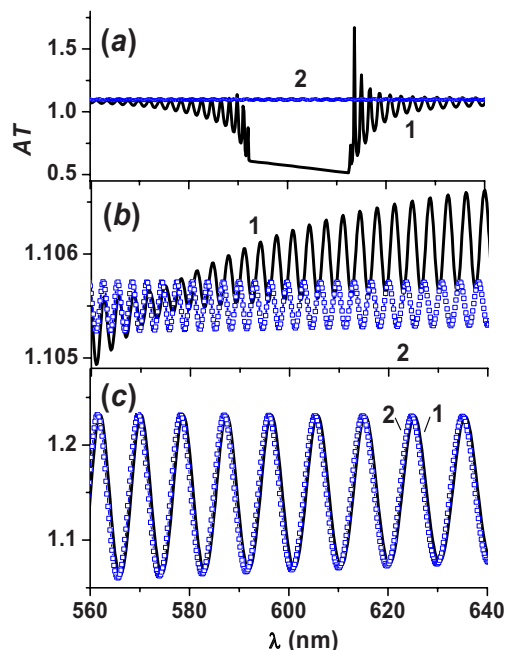

FIG. 6. (Color online) Calculated spectra of amplified transmission for two materials at three different angles of p-polarized beam propagation $\beta_p=0$ (plot a), 40° (plot b), and 70° (plot c). Numbers 1 and 2 at the curves are related to chiral CLC structure and uniform nematic structure, respectively.

beam, partially reflected at the second boundary (in points A, B, etc.), leaves the liquid crystal for the prism. Its intensity, i.e., amplified transmission coefficient AT$=I_{out}/I_{in}$, is calculated as a function of the wavelength, incident angle, polarization, and relevant parameters of the media (thickness of a liquid crystal, refraction indices, and gain coefficients). Even 50 nm thick polyimide alignment layers with $n_{PI}=1.6$ are taken into account.

At first, the calculations of the AT spectra have been carried out for our CLC material with the helical axis perpendicular to the boundaries. All parameters of the CLC are taken from experiment (see above) except the gain coefficient $-\alpha_\perp$ taken to be slightly exceeding a threshold value: $-\alpha_\perp(CLC)=0.001$ μm^{-1} and $-\alpha_\parallel(CLC)=0.003$ μm^{-1} (the ratio $\alpha_\parallel/\alpha_\perp=3$ is also taken from the experiment). The refraction index $n_0=1.515$ is assumed to be the same for both the prism and the glass. The curves marked by solid lines (curve 1) in Figs. 6(a)–6(c) show the modeled spectra of the helical CLC structure for three different incidence angles of the probe beam $\beta_0=0°$, 40°, and 70°, respectively.

The uniform structure was modeled by a virtual nematic liquid crystal with refraction indices $n_\parallel=1.478$ and $=n_\perp=1.5057$ (for our CLC these indices correspond to directions $\parallel$ and $\perp$ to the helical axis, respectively). The gain coefficient of the nematic was also properly adjusted to the CLC indices: $-\alpha_\parallel=0.001$ and $-\alpha_\perp=0.002$ μm^{-1}. The line-symbol curves (curve 2) in Fig. 6 correspond to a uniform nematic structure. All the AT curves in Fig. 6 are calculated for the p-polarized probe beam.

At the normal incidence $\beta_0=0$ (plot a) the amplified transmission (curve 1) shows all the features of the Bragg diffraction absent in the AT spectrum of the nematic (curve 2). With increasing β_0 the stop band shifts to the UV region

and we observe only Fabry–Pérot oscillations. At $\beta_0=40°$ there is still a substantial difference in the AT spectra for two materials (curves 1 and 2 in plot *b*). This difference becomes negligible at $\beta_0=70°$ (plot *c*). With further increasing β_0, a singularity in AT (lasing) appears in both models at the same angle of 76.9° and the same wavelength. In fact, in the range of angles $70°<\beta_0<90°$ the QIPL modes are completely decoupled from the BM and we may consider optical properties of a CLC to be equivalent to those of the optically negative nematic (it was verified for both *s* and *p* polarizations). This angular range meets our needs for calculation of the threshold gain of the QIPL modes. Since the analytical approach is more general and less time consuming we shall apply it to what follows below.

IV. THRESHOLD GAIN COEFFICIENT FOR QIPL MODE LASING

In the analytic approach,[12] one deals with a nematic layer of thickness *d* (in the *z*-direction) that is much less than the layer dimensions in the *x*- and *y*-directions. The threshold conditions for the laser generation on the QIPL modes are found by comparison of the gain on the down-up path AB (see Fig. 5) with losses due to transmission (leakage) of energy into the neighbor glasses. The feedback is provided by the Fresnel reflections at the two boundaries. These reflections are especially strong (close to 1) for the beams propagating at the angles $\beta_{s,p}$ close to 90°. Now, the probe beam is not necessary, any fluctuation of the field within the amplifying layer may be considered as a seed beam. The results of the consideration of the threshold gain (negative absorption) $-\alpha_\perp^*$ for a homeotropically oriented nematic liquid crystal, both optically positive and negative are summarized as follows:

$$-\alpha_\perp^*(\beta_0) = \frac{\cos\left(\text{asin}\dfrac{n_0 \sin \beta_0}{n_\perp}\right)}{d}$$
$$\times \ln\left[\frac{\sin\left(\text{asin}\dfrac{n_0 \sin \beta_0}{n_\perp}+\beta_0\right)}{\sin\left(\text{asin}\dfrac{n_0 \sin \beta_0}{n_\perp}-\beta_0\right)}\right]^2, \quad (1)$$

for the *s*-polarized wave and

$$-a_\perp^*(\beta_0) = \frac{\cos[\beta_p(\beta_0)]}{d[A^{-1}K_D \sin^2 \beta_p(\beta_0) + B^{-1}\cos^2 \beta_p(\beta_0)]}$$
$$\times \ln\left\{\frac{\tan[\beta_0+\beta_p(\beta_0)]}{\tan[\beta_0-\beta_p(\beta_0)]}\right\}^2, \quad (2)$$

for the *p*-polarized wave.

Here, β_s and β_p are propagation angles of *s*- and *p*-modes, β_0 is the angle of the outgoing beam in the prism in accordance with Fig. 5, and
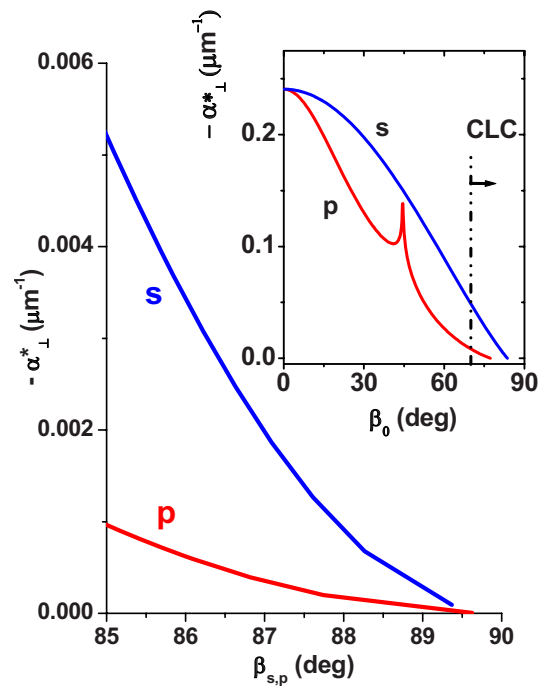

FIG. 7. (Color online) Inset: calculated threshold gain $-\alpha_\perp^*$ for the *s*- and *p*-modes propagating in the uniform nematic structure as a function of angle β_0 in the prism (the vertical dash-dot line shows the limit of the graph application to CLC structure, $\beta_0>70°$). Main plot: the same gain curves plotted as functions of the mode propagation angles $\beta_{s,p}$ within the liquid crystal (here, the range of $\beta_{s,p}$ is valid for both the nematic and CLC structures).

$$A = \sin^2 \beta_p(\beta_0) + \left(\frac{n_\parallel}{n_\perp}\right)^4 \cos^2 \beta_p(\beta_0),$$

$$B = \cos^2 \beta_p(\beta_0) + \left(\frac{n_\perp}{n_\parallel}\right)^4 \sin^2 \beta_p(\beta_0),$$

$$K_D = \frac{\alpha_\parallel}{\alpha_\perp},$$

(3)

$$\beta_p(\beta_0) = \text{asin}\{n_0 n_\parallel [n_\parallel^2 n_\perp^2 + n_0^2(n_\parallel^2-n_\perp^2)\sin^2 \beta_0]^{-1/2}\sin \beta_0\}.$$

In our case, the refraction index of the prism (and glass) is $n_0=1.515$, the indices of the nematic are $n_\parallel=1.478$, $n_\perp=1.5057$, $K_D=3$, and layer thickness is $d=48$ μm. The results of the threshold gain calculation for the *s*- and *p*-modes as a function of angle β_0 in prism are shown in the inset of Fig. 7. The spike in the *p*-curve corresponds to the Brewster angle of 44.5° at the nematic-glass interface. We see the same tendency for both curves: with increasing β_0 the threshold gain decreases to zero at limiting angles $\beta_0(s) \rightarrow 83.6°$ and $\beta_0(p) \rightarrow 77.2°$ (corresponding to the propagating angles $\beta_{s,p} \rightarrow 90°$ in the liquid crystal). The threshold gain decrease is a consequence of a dramatic increase in both the amplifying down-up path AB and the Fresnel reflections responsible for the laser feedback. In fact, these reflections provide an angular selectivity of the Fabry–Pérot structure for QIPL modes with largest $\beta_{s,p}$.

The results shown in the inset of Fig. 7 may safely be applied to our CLC only for angles $\beta_0=70°-90°$, as shown

in Sec. III. Now we can see that the limiting angles for the thresholdless lasing on the QIPL modes fall into the range of our experimental accuracy for angles $\beta_0(s)=83.4\pm0.4°$ and $\beta_0(p)=77.4\pm0.4°$ found earlier in Fig. 3. It means that in the experiment we deal with the QIPL modes propagating at angles $\beta_{s,p}$ in the liquid crystal very close to 90°. The main plot in Fig. 7 shows the same threshold gain curves plotted as functions of the angles $\beta_{s,p}$ in the CLC layer, $\beta_{s,p}=(n_0/n_{s,p})\beta_0$, where $n_s=n_\perp=1.5057$ and

$$n_p(\beta_p) = n_\parallel n_\perp (n_\parallel^2 \cos^2\beta_p + n_\perp^2 \sin^2\beta_p)^{-1/2}. \quad (4)$$

Using the main plot in Fig. 7 we can estimate the threshold gain for our QIPL modes. To this effect, we shall find those eigenmodes, which can propagate in CLC at angles close to 90°.

V. MODE STRUCTURE

The previous consideration is applied to the continuous spectrum of possible modes depending on the cell thickness, light wavelength, and mode angles. The discrete eigenmodes in the Fabry–Pérot structure satisfy to the well-known conditions for the beam constructive interference,

$$2n_s d \cos\beta_s = m\lambda_0 \quad (s\text{-mode}),$$

$$2n_p(\beta_p)d \cos\beta_p = m\lambda_0 \quad (p\text{-mode}). \quad (5)$$

Here, $d=48$ μm, $n_s=1.5057$, and n_p is defined by Eq. (4). Now we shall fix the number $m=1-15$ of the lowest modes and confine the wavelengths to the range of $\lambda=601-613$ nm, within which lasing is observed on the QIPL modes (see Fig. 3) (now the BM at $\lambda=622.3$ nm is out of consideration). Then, from Eq. (5) we obtain a plot related to the wavelength of a particular eigenmode to its propagation angle β_s (plot a) or β_p (plot b) (see Fig. 8). The pairs of horizontal dash-dot lines limit the wavelength range we are interested in.

Figure 8 gives us a clear map of all the eigenmodes propagating at large angles in the range of $86°<\beta_{s,p}<90°$. For the s-polarization the lowest number (and lowest threshold) modes are marked by solid symbols (diamond and circle). They have numbers $m=5$ and 7, respectively. For the p-polarization the lowest modes have larger numbers, $m=9$, 11, and 13, shown by solid rectangular, star, and hexagon, respectively. The threshold gain for these modes can be found from the main plot in Fig. 7. The results are collected in Table I.

From the table we see that two s-polarized lasing modes with numbers 5 and 7 propagate in prism at the angles (β_0) overlapping the experimental angle within accuracy of measurements. The wavelengths of the two calculated modes ($\lambda=605.5$ and 612.6 nm) are very close to those ($\lambda=604$ and 610 nm) observed in the experiment [see Fig. 4(a)]. Three p-modes propagate at β_0 angles, which are also very close to the experimental one and their wavelengths are in agreement with the bands at $\lambda=603$, 607, and 611 nm seen in Fig. 4(b). The discrepancy can easily be accounted for by some irregularity in the cell thickness. The single mode lasing observed in the experiment with oblique incidence of pump light
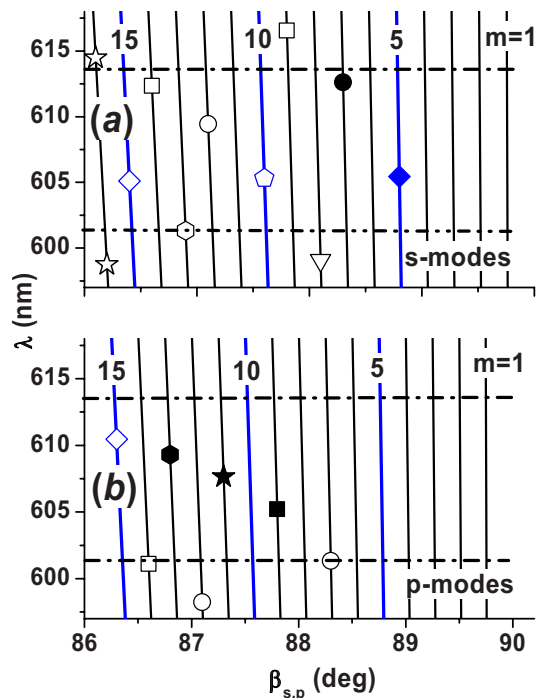

FIG. 8. (Color online) The angular and spectral positions of the s-(plot a) and p-(plot b) eigenmodes found from Eq. (5) with experimental values of the cell thickness and refraction indices. Mode numbers are shown on the top of each plot. Horizontal dash-dot lines show the range of λ in which the QIPL lasing modes are observed in experiment.

($\theta=45°$) could also be understood: in that case, the x-dimension of the pump spot is $\sqrt{2}$ times longer and since the strongest line is always amplified stronger, the weaker lines become hardly visible.

The range of the calculated principal component of the threshold gain coefficient perpendicular to the director is $-\alpha_\perp^* \approx (2-7)\times10^{-4}$ μm^{-1}, i.e., about 2–7 cm^{-1}, for all modes in Table I. The values of the principal component parallel to the director should be somewhat less, because the positive ratio $K_D=3$ is in the denominator of Eq. (2). The experimental threshold pump fluence for lasing on both s- and p-QIPL modes in our CLC is about $W_p^*=0.13$ mJ/cm^2. This quantity allows us to estimate the corresponding gain using results of other experiments. For instance, in experiments with the same concentration of DCM in nematic mixture E7 we have obtained gain of about 2–3 cm^{-1} at an enhanced fluence $W_p=0.7$ mJ/cm^2 but, in that case, an effect of the gain saturation is not excluded.[15] For the same concentration of Rhodamine-645 dye in glycerin, at the pump fluence of 0.13 mJ/cm^2, we have found the gain coefficient of about 10 cm^{-1} without saturation (see Fig. 13 of Ref. 16). The positive absorption coefficient of rhodamine-645 at the pump wavelength of 532 nm is two to three times higher than that of DCM; therefore, we may expect the value of $-\alpha=3-5$ cm^{-1} for DCM at 0.13 mJ/cm^2 (to be compared with 2–7 cm^{-1} found in Fig. 7). Therefore, our calculations of the threshold gain are in reasonable agreement with other experiments.

We would also like to make a comment on the role of a waveguiding regime. We have also studied a dye-doped CLC with refraction indices exceeding the indices of the prism

TABLE I. QIPL mode numbers m, propagation angles in CLC ($\beta_{s,p}$) and in prism (β_0), lasing wavelength (λ), and the threshold principal gain coefficient $-\alpha_\perp^*$ for s- and p-polarizations of the modes.

Polarization	m	$\beta_{s,p}$ (deg)	β_0 (deg)	λ (nm)	$-\alpha_\perp^*$ (μm^{-1})
s	5	88.8	83.5	605.45	4.2×10^{-4}
	7	88.3	83.4	612.6	6.6×10^{-4}
Expt. (s)			83.4 ± 0.4		
p	9	87.8	77.1	605.2	1.9×10^{-4}
	11	87.3	77.0	607.6	3.6×10^{-4}
	13	86.8	76.9	609.3	4.2×10^{-4}
Expt. (p)			77.4 ± 0.4		

and the glass. In that case, there is a waveguiding effect and the eigenmodes with the lowest mode numbers (and potentially lowest threshold for lasing) remain in the waveguide. Therefore, the lasing appears on that leaky mode, which propagates in the CLC at an angle $\beta_{s,p}$ slightly smaller than the total reflection angles at the boundary between the prism and liquid crystal, as was noticed earlier.[8] This limitation, however, would make an additional selection of a lasing mode, favorable for the single mode lasing.

Finally, note that our model for the gain calculation is basically very simple, it is just a Fabry–Pérot structure. However, the leaky modes sliding along the glass-liquid crystal boundary could, in principle, be additionally coupled to the evanescent waves penetrating into the glass from the excited liquid crystal with inversed population. Such a coupling would increase the gain for the leaky modes in analogy with the amplified total internal reflection from an excited medium[17] and the amplification of gallery whispering modes in nonexcited spherical droplets surrounded by excited medium.[18]

VI. CONCLUSION

In conclusion, using a cell consisting of a prism and a flat glass, we have carried out the measurements of the angles, at which QIPL laser modes propagate within a thin layer of a CLC doped with a laser dye. Such modes are generated in CLC due to strong Fresnel reflections from the glass boundaries at propagation angles $\beta_{s,p}$ very close to 90°. Both the prism and the glass have refraction indices higher than relevant CLC indices, therefore the waveguide effect is excluded. In the experiment, two groups of modes going out of the prism and polarized differently (s and p) have been found. Using the modeling based on the precise numerical solution of the Maxwell equations we have shown that, at the angles of $\beta_{s,p} > 70°$, the helical structure of a CLC has the same optical properties as an equivalent optically negative, uniform nematic structure. This allowed us to use the known analytical approach for the uniform nematic for calculations of the threshold gain for the leaky modes in the helical CLC studied. The gain has been found for the particular eigen-

modes, whose propagation angles coincide with experimental ones. Generally, all the experimental and theoretical data are in good agreement and the behavior of the QIPL lasing modes is much better understood at the quantitative level.

[1]L. M. Blinov, *Electro-Optical and Magneto-Optical Properties of Liquid Crystals* (Wiley, Chichester, 1983), Fig. 2.10.

[2]I. Il'chishin, E. Tikhonov, V. Tishchenko, and M. Shpak, JETP Lett. **32**, 24 (1980).

[3]V. I. Kopp, Z.-Q. Zhang, and A. Genack, Prog. Quantum Electron. **27**, 369 (2003).

[4]H. Finkelmann, S. T. Kim, A. Muñoz, P. Palffy-Muhoray, and B. Taheri, Adv. Mater. (Weinheim, Ger.) **13**, 1069 (2001).

[5]A. Chanishvili, G. Chilaya, G. Petriashvili, R. Barberi, R. Bartolino, G. Cipparrone, A. Mazzulla, R. Gimenes, L. Oriol, and M. Pinol, Appl. Phys. Lett. **86**, 051107 (2005).

[6]J. Schmidtke, W. Stille, and H. Finkelmann, Phys. Rev. Lett. **90**, 083902 (2003).

[7]G. Strangi, V. Barna, R. Caputo, A. de Luca, C. Versace, N. Scaramazza, C. Umeton, R. Bartolino, and G. Price, Phys. Rev. Lett. **94**, 063903 (2005).

[8]L. M. Blinov, G. Cipparrone, V. Lazarev, A. Mazzulla, and P. Pagliusi, Appl. Phys. Lett. **89**, 031114 (2006).

[9]L. M. Blinov, G. Cipparrone, A. Mazzulla, P. Pagliusi, and V. Lazarev, J. Appl. Phys. **101**, 053104 (2007).

[10]R. Jakubiak, T. J. Bunning, R. A. Vaia, L. V. Natarajan, and V. P. Tondiglia, Adv. Mater. (Weinheim, Ger.) **15**, 241 (2003).

[11]A. Penzkofer, W. Holzer, H. Tillmann, and H.-H. Hörhold, Opt. Commun. **229**, 279 (2004).

[12]S. P. Palto, JETP **103**, 472 (2006).

[13]S. P. Palto, JETP **92**, 552 (2001).

[14]S. P. Palto, Crystallogr. Rep. **48**, 124 (2003).

[15]L. M. Blinov, G. Cipparrone, V. V. Lazarev, P. Pagliusi, and T. Rugiero, Opt. Express **16**, 6625 (2008).

[16]L. M. Blinov, G. Cipparrone, V. V. Lazarev, P. Pagliusi, T. Rugiero, and B. A. Umanskii, J. Nonlinear Opt. Phys. Mater. **16**, 519 (2007).

[17]B. Ya. Kogan, V. M. Volkov, and S. A. Lebedev, Pis'ma Zh. Eksp. Teor. Fiz. **15**, 144 (1972).

[18]V. V. Datsyuk, S. Juodkazis, and H. Misava, J. Opt. Soc. Am. B **22**, 1471 (2005).